

Advances in halide perovskite semiconductors for energy-integrated and energy-resolved X-ray detection

Yibin LAI, Yang (Michael) YANG

Cite this as: Yibin LAI, Yang (Michael) YANG, 2024. Advances in halide perovskite semiconductors for energy-integrated and energy-resolved X-ray detection. *Journal of Zhejiang University-SCIENCE A (Applied Physics & Engineering)*, 25(10):824-840. <https://doi.org/10.1631/jzus.A2300660>

Interaction of X-rays and γ -rays with matter

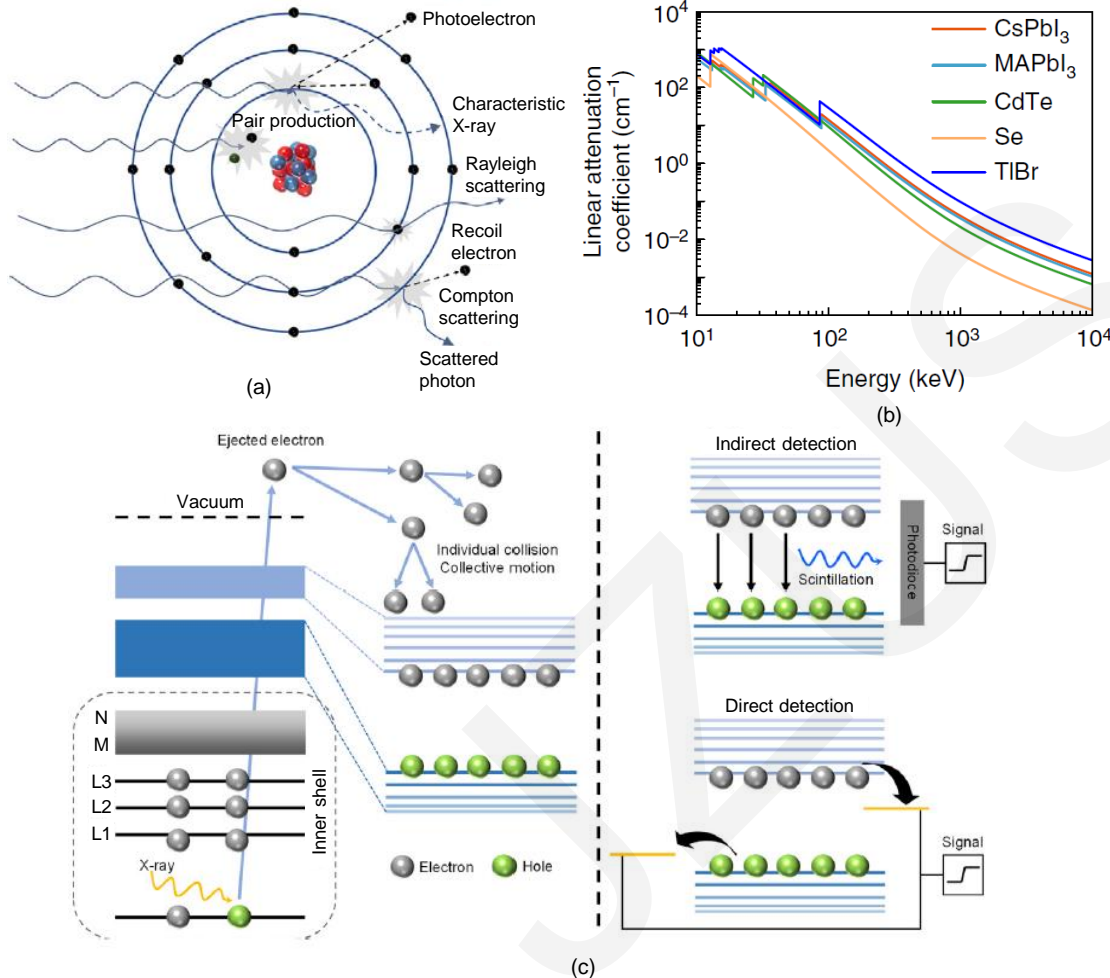


Fig. 1 (a) Processes by which X-ray (γ -ray) photons interact with matter: photoelectric absorption, Rayleigh scattering, Compton scattering, and pair production; (b) Linear attenuation coefficient for various materials; (c) Mechanism of electron-hole generation in semiconductors under X-rays (γ -rays) and the mechanisms of indirect and direct detections.

Wu, H. et al, *Matter* **4**, 144-163, (2021).

Wei, H. & Huang, J. *Nature Communications* **10**, 1066, (2019).

Direct detection of X-rays and γ -rays

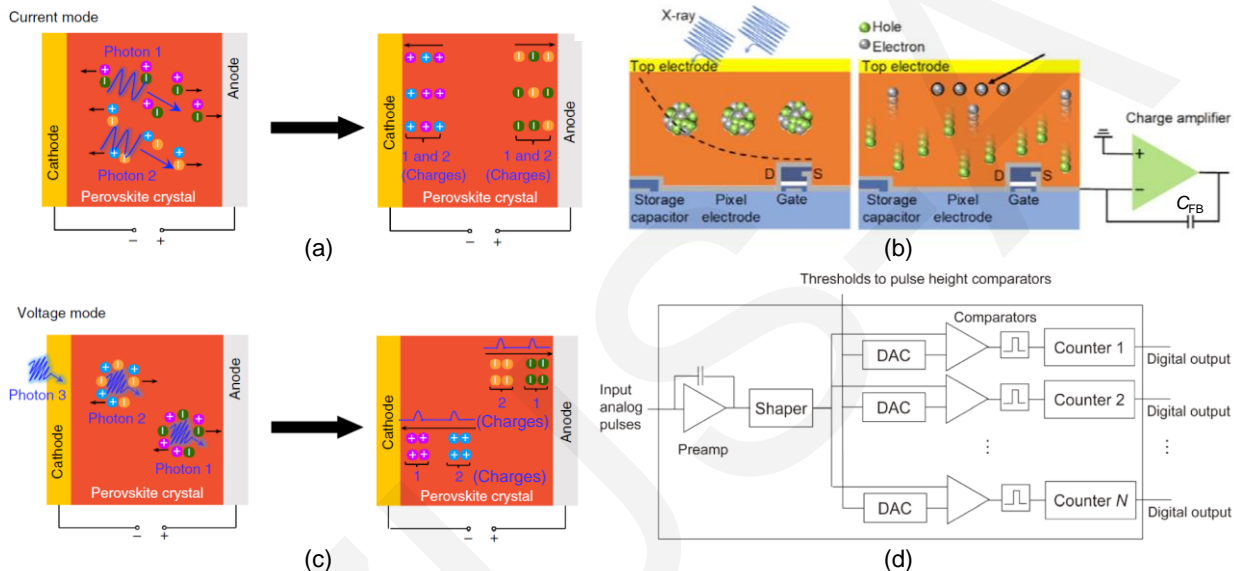


Fig. 2 (a) Mechanism by which energy integrating detectors (EIDs) work in the current mode; (b) Device configuration of EIDs; (c) Mechanism by which photon counting detectors (PCDs) work in voltage mode; (d) Schematic diagram of the application-specific integrated circuit (ASIC) .

Wu, H. et al, *Matter* **4**, 144-163, (2021).

Wei, H. & Huang, J. *Nature Communications* **10**, 1066, (2019).

Taguchi, K. & Iwanczyk, J. S. *Medical Physics* **40**, 100901, (2013).

Development of perovskite EIDs

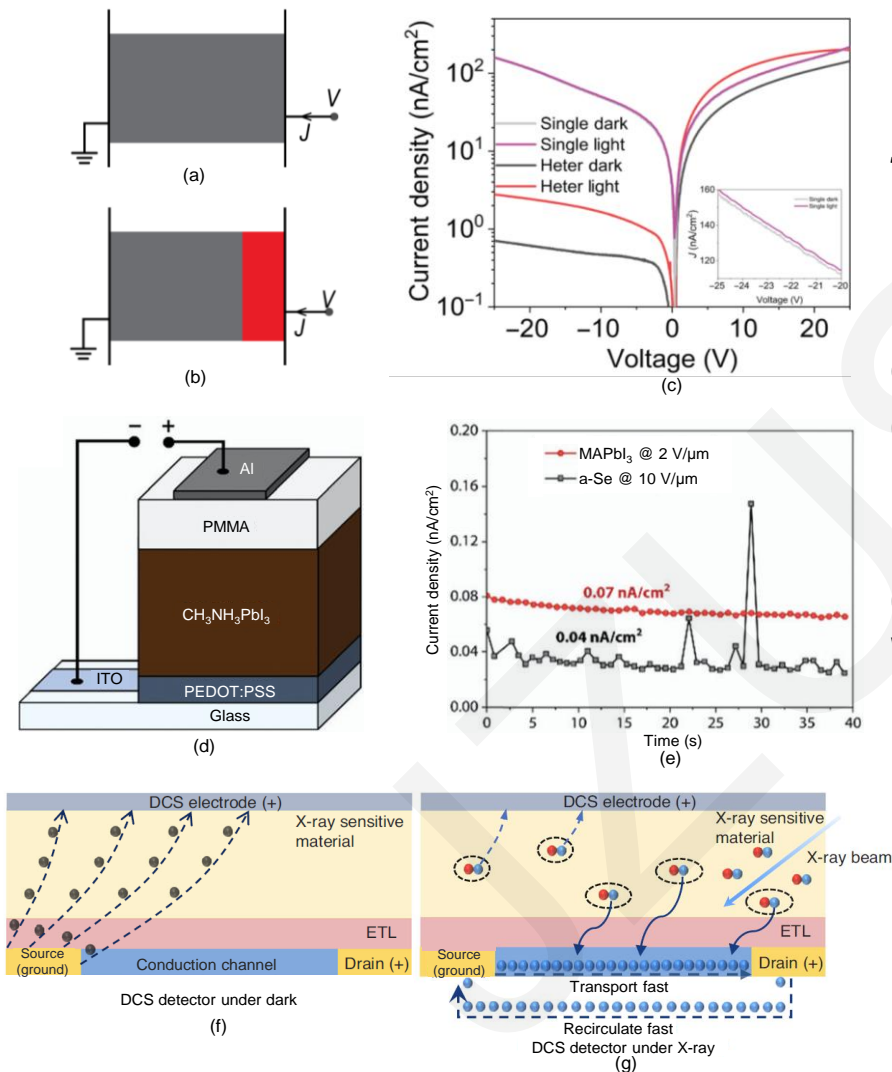


Fig. 3 (a) Schematic of a single junction device; (b) Schematic of heterojunction device; (c) Device performance of single junction and heterojunction device; (d) Schematic diagram of the PMMA inserted EIDs; (e) Dark current density of MAPbI₃ EIDs and a-Se EIDs; (f) Working mechanism of dark-current-shunting (DCS) detector under dark (g) Working mechanism of DCS detector under X-ray.

Zhou, Y. et al, Science Advances 7, eabg6716, (2021).

Li, Y. et al, Journal of Materials Chemistry C 10, 1228-1235, (2022).

Jin, P. et al, Nat Communication 14, 626, (2023).

Development of perovskite PCDs

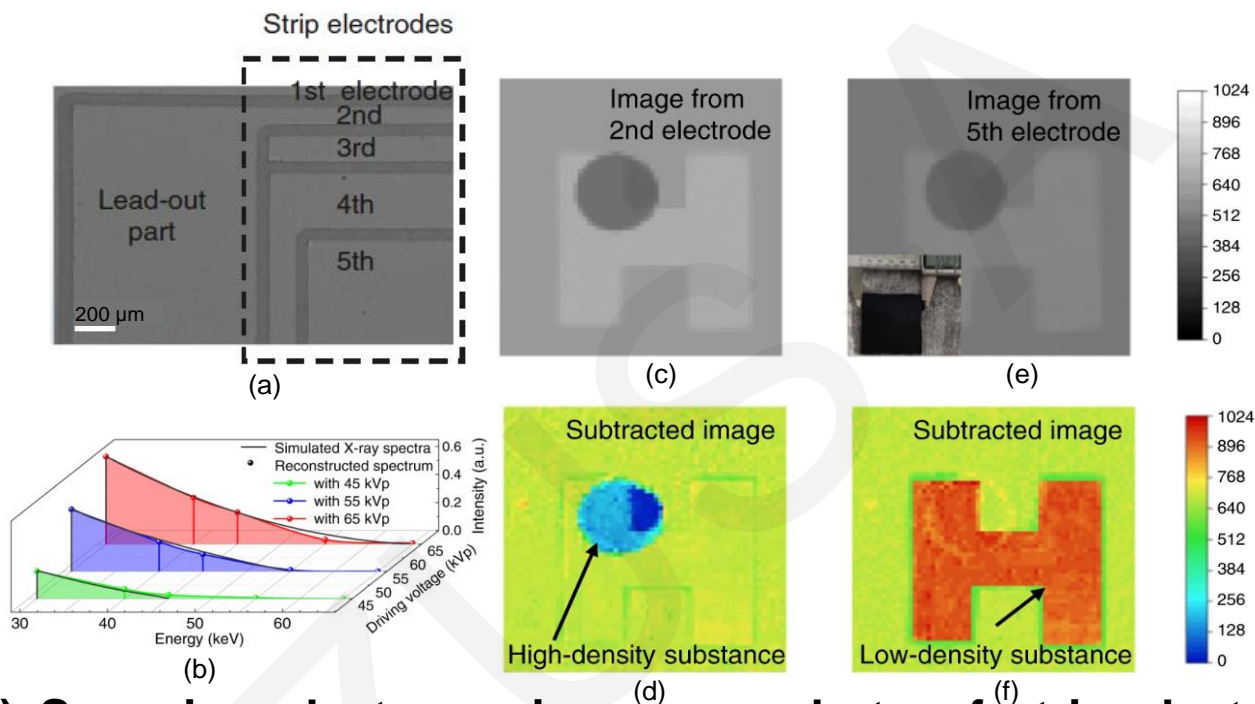


Fig. 4 (a) Scanning electron microscope photo of strip electrodes; (b) Simulated X-ray spectra and reconstructed spectrum when the driving voltages of the X-ray tube were 45, 55, and 65 kVp; (c) Image of the artificial sample from the 2nd electrode; (d) Subtracted image of a high-density substance CaCO₃ tablet; (e) Image of the artificial sample from the 5th electrode; (f) Subtracted image of a low-density substance paraffin 'H' letter.

Development of perovskite PCDs

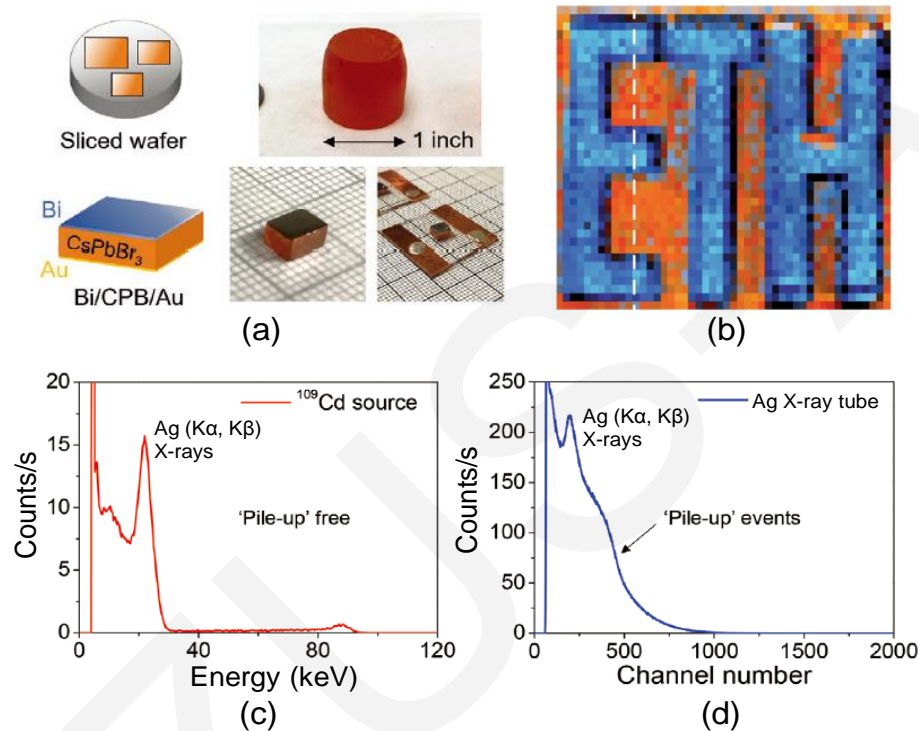


Fig. 5 (a) Wafer grown from Bridgman method and device configuration of CsPbBr₃; (b) Energy-resolved image of the characters 'ETH'; (c) Spectrum of the ¹⁰⁹Cd source measured by the CsPbBr₃ detector; (d) Spectrum of the Ag X-ray tube measured by the CsPbBr₃ detector. ◦

He, Y. *et al*, *Advanced Functional Materials* **32**, 2112925, (2022).

Sakhatskyi, K. *et al*, *Nature Photonics* **17**, 510-517, (2023).